# Formation and stability of rocksalt ZnO nanocrystals in MgO

S. W. H. Eijt,[a] J. de Roode, and H. Schut
*Radiation, Radionuclides and Reactors, Faculty of Applied Sciences, Delft University of Technology, Mekelweg 15, 2629 JB Delft, The Netherlands*

B. J. Kooi and J. Th. M. De Hosson
*Department of Applied Physics, Zernicke Institute for Advanced Materials, University of Groningen, Nijenborgh 4, 9749 AG Groningen, The Netherlands*

(Received 4 October 2007; accepted 22 October 2007; published online 13 November 2007)

Coimplantation of Zn and O ions into a single crystalline MgO and subsequent thermal annealing were applied in the synthesis of ZnO nanocrystals. Electron microscopy showed that rocksalt instead of wurtzite ZnO stabilizes for relatively large nanocrystals up to ~15 nm, resulting from its small lattice mismatch with MgO of ~1.7%. The vacancies initially created by implantation induce favorable nanocrystal growth kinetics and are effectively absorbed during the nucleation and growth processes. The optical band edge of the ZnO nanocrystals was detected at ~2.8 eV.
 [DOI: 10.1063/1.2809651]

ZnO is an interesting wurtzite II-VI semiconductor with a favorable optical band gap of ~3.3 eV.[1] Both *n*- and *p*-type doping have recently been accomplished, making this cheap compound a promising candidate as substitute for III-V semiconductors such as GaN in blue lasers and other (opto-)electronic devices. Alloys of ZnO with MgO form wurtzite solid solutions for Mg concentrations up to ~30%, resulting in an increase in optical band gap to ~3.9 eV.[2,3] At Mg concentrations above ~45%, rocksalt $Mg_{1-x}Zn_xO$ solid solutions are stabilized for deposited thin films,[2–4] and can be tailored in band gap in the deep-ultraviolet range between ~4.8 eV for $x \sim 0.55$ up to ~7.8 eV for MgO. ZnO is polymorphic and it is known to exist in two cubic structures. Stabilization of a rocksalt ZnO phase can be achieved as a result of external pressure.[5,6] Furthermore, ZnO also exists in a metastable sphalerite structure. The wurtzite and sphalerite arrangements are very much alike, with the wurtzite phase slightly more stable at about the same equilibrium density.[7] Rocksalt ZnO is characterized by a significant ~0.8 eV /formula unit[7] smaller equilibrium cohesive energy at a ~25% higher density. Stabilization of a rocksalt phase in general may also occur for nanocrystals (NCs) typically in the range of 1–10 nm as a result of the increasingly important influence of surfaces for colloidal quantum dots[8–10] or of interfaces for NCs embedded in the host matrices.[11,12] The use of nanoparticles further leads to a size-dependent increase in optical band gap.[8,13] Synthesis of ZnO NCs embedded in MgO can therefore pave the way to extending the tunability of the rocksalt band gap by including the blue-violet to ultraviolet range between ~3 and ~5 eV.

A promising all-solid-state synthesis route for compound NCs consists of sequential implantation of both types of ions and subsequent thermal annealing,[11,14] which is particularly interesting because the passivation of surface states can be achieved robustly by incorporation of the NCs in a wide band gap material such as MgO. Previous studies[15] approached the synthesis of embedded ZnO NCs using high dose $Zn^+$ ion implantation in MgO(100) single crystals followed by thermal annealing under oxidizing conditions. However, this leads to the formation of metallic Zn NCs exclusively,[15] with interesting optical properties related with a pronounced Mie scattering resonance. Coimplantation of Zn and O ions, on the other hand, will directly lead to a situation of local supersaturation for both types of ions and is therefore a promising candidate for the synthesis of embedded ZnO NCs.

MgO(100) single crystals were implanted using 40 keV $O^+$ and 140 keV $Zn^+$ ions at a dose of $1\times10^{17}$ ions/cm$^2$ each. The stopping and range of ions in matter (SRIM) calculations[16] showed that maximum Zn and O concentrations of ~20 and 17 at % were reached at a depth of 62 and 66 nm, respectively, after implantation [see inset of Fig. 1(a)]. The evolution of the implanted samples was monitored after each subsequent thermal annealing treatment for 0.5 h in the temperature range between 570 and 1370 K, using temperature steps of 100 K. The Doppler broadening of annihilation radiation[10,15,17,18] (511 keV) was measured using positrons with a kinetic energy in the range of 0–25 keV corresponding to average positron implantation depths up to ~1.9 $\mu$m. Optical absorption spectra (OAS) were collected in the range of 1.5–6.5 eV. Cross-sectional transmission electron microscopy (TEM) was performed on two selected coimplanted samples after the 970 K step. A JEOL 4000 EX/II electron microscope was used, operating at 400 kV with a point resolution of 0.17 nm. The specimen preparation was discussed elsewhere.[19] In order to facilitate comparison with the formation of Zn-clusters,[15] an additional set of samples was implanted in the same batch with $Zn^+$ ions only and annealed simultaneously with the coimplanted samples.

Figure 1(a) shows representative positron depth profiles of the Doppler *W* and *S* parameters for the Zn and Zn plus O coimplanted samples after the annealing step at 770 K, using momentum windows of $8.2\times10^{-3}\ m_oc<|p|<23.4\times10^{-3}\ m_oc$ and $|p|<3.0\times10^{-3}\ m_oc$ for *W* and *S*, respectively.[10] While *W* provides a measure for positron annihilation with semicore electrons,[10,17] providing chemical sensitivity to the positron trapping site, *S* is a measure of annihilation with valence electrons, providing sensitivity to the electronic structure and the presence of vacancies.[17] In the *S*-*W* diagram [Fig. 1(b)] the characteristic *S*-*W* points

[a]Electronic mail: s.w.h.eijt@tudelft.nl

 

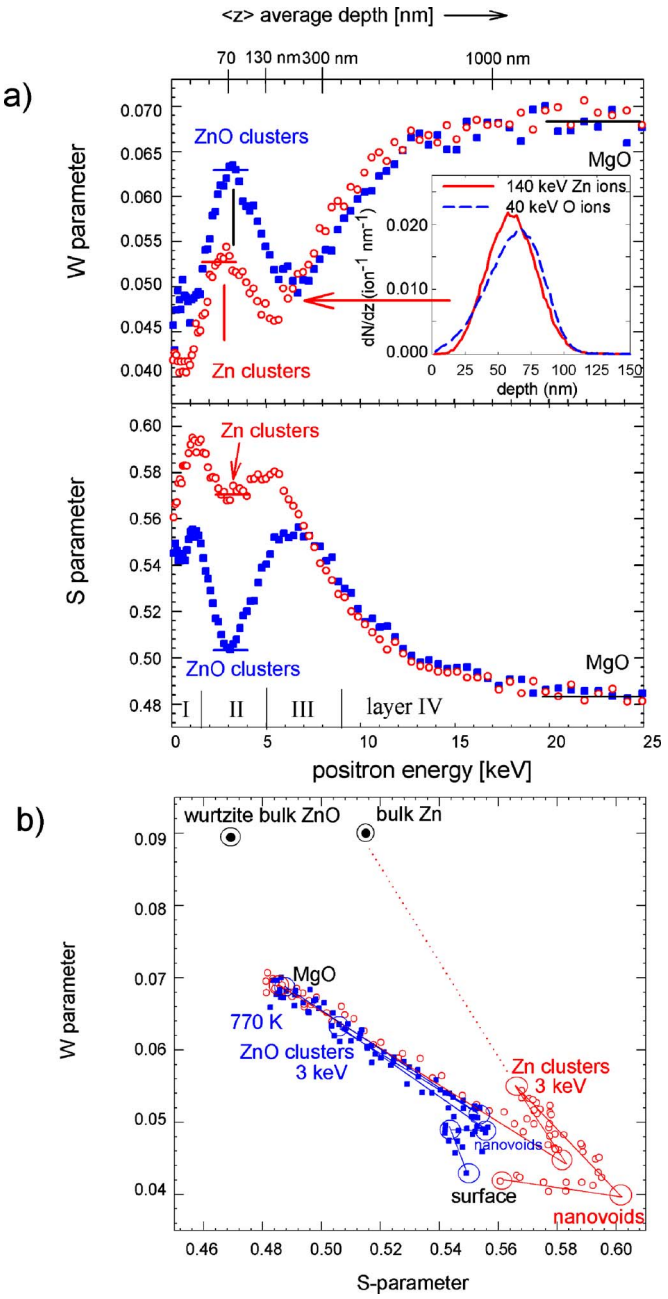


FIG. 1. (Color online) (a) Doppler *S*- and *W*-parameter depth profiles of Zn respectively Zn and O implanted MgO, annealed at 770 K: region (I) pre-implantation defects, region (II) layer containing Zn or ZnO NCs, region (III) nanovoid formation by knock-on damage, and region (IV) pristine MgO. The inset shows the calculated implantation profiles of Zn and O ions, respectively. (b) *S*-*W* diagram of the Zn and Zn plus O implanted samples, annealed at 770 K.

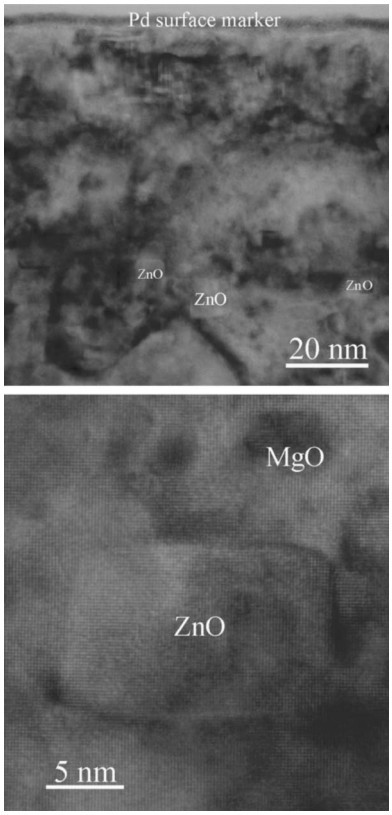


FIG. 2. (a) Bright-field transmission electron microscopy image of a Zn and O implanted MgO(100) layer annealed at 970 K. In the depth range between ~45 and ~85 nm below the MgO surface, nearly rectangular shaped embedded ZnO NCs are discerned, where a few have been indicated. (b) High-resolution TEM image of an embedded rocksalt ZnO nanocrystal showing lattice matching with the surrounding MgO.

determined for bulk crystalline MgO, wurtzite ZnO, and metallic Zn are included, showing that the presence of Zn(3*d*) electrons leads to a substantially larger value for *W*.

The *W* and *S* parameter depth profiles are seen to follow quite neatly the ion implantation profiles shown in the inset of Fig. 1(a). First, the growth of ZnO (or Zn) NCs requires high ionic mobility and lattice relaxations, in which the vacancies initially formed by the ion implantation are effectively absorbed, leading to low vacancy concentrations in layer II. This is in striking contrast to the pre- and postimplantation layers I and III, where the high *S* and small *W* parameters show that nanovoids are formed during thermal annealing by clustering of the implantation-induced vacancies.[15,20] Further, in the *S*-*W* diagram, the cluster point at 3 keV for the Zn-implanted sample annealed at 770 K clearly points in the direction of the characteristic point for metallic Zn, signaling the presence of Zn NCs. The calculated positron affinity of Zn (−5.24 eV[21]) is quite close to that of MgO (−5.5 eV[22]), indicating that positrons trap, most likely, into vacancies formed at the nonlattice matching Zn‖MgO interfaces rather than into the Zn NCs themselves. The *S*-*W* point at 3 keV for coimplanted samples, in contrast, is strongly shifted from the Zn NCs *S*-*W* point, demonstrating that Zn-related NCs are not formed. Instead, ZnO NCs are formed due to their higher cohesive energy. The position of the *S*-*W* point close to bulk MgO suggests, however, that positrons annihilate primarily in nearly defect-free MgO, indicating that ZnO NCs themselves do not form a positron trapping site in MgO. We note that positron trapping in Zn vacancies ($V_{Zn}$) in wurtzite ZnO (Ref. 23) would correspond to a *S*-*W* cluster point of approximately ($S \sim 0.49$, $W \sim 0.071$), i.e., also rather close to MgO. However, the presence of wurtzite ZnO NCs was not observed here.

Our TEM study provided a clear proof for the formation of embedded ZnO NCs adopting the rocksalt structure exclusively. The presence of nearly rectangular nanocrystals can be discerned in bright-field TEM images in the depth interval between ~45 and 85 nm below the surface of the coimplanted MgO sample annealed at 970 K [Fig. 2(a)]. This depth-interval coincides with the region of high Zn-concentration as determined from *in situ* energy dispersive x-ray analysis and SRIM calculations. High-resolution im-

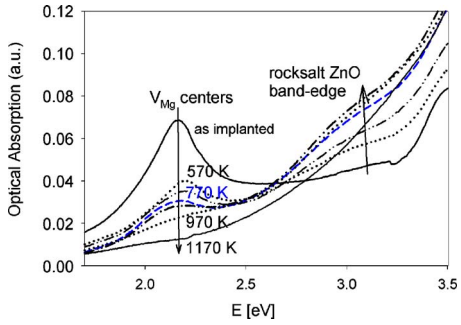


FIG. 3. Optical absorption spectra of a coimplanted MgO(100) sample vs annealing temperature in the range of 570–1170 K. The ZnO band edge grows at ~2.8 eV, signaling growth of the nanocrystals, leading in parallel to the disappearance of Mg vacancies ($V_{Mg}$). At 1170 K, the band edge absorption disappears upon dissociation of the ZnO NCs.

ages [Fig. 2(b)] reveal that the NCs have a rocksalt crystal structure with a lattice constant matching that of the surrounding MgO, consistent with reported lattice constants of ~4.28 (Refs. 4 and 6) and 4.212 Å for rocksalt ZnO and MgO, respectively. While the NCs are generally nearly rectangular in shape, it is noteworthy that their corners are rounded. Their morphologies are thus intermediate the rectangular shape observed for solid Kr NCs[24] and nanovoids[19] in MgO and the almost spherical shape of Au NCs[25] and of equally large wurtzite CdSe NCs[11] in MgO. Further, a striking observation is that the rocksalt ZnO phase remains stable relative to wurtzite for NC sizes typically in the range of up to at least ~15 nm, i.e., clearly larger than for rocksalt CdSe NCs embedded in MgO.[11] This shows that the improved lattice matching and correspondingly low interface energies are at the origin of stabilization of rocksalt NCs in MgO.[11,12] A mechanism based on pressure exerted by the MgO host[24] can be excluded since the transition pressures for ZnO and CdSe of ~9 (Refs. 6 and 7), and ~3 GPa (Refs. 8 and 26), respectively, have the opposite order than required in that case. Neither features related to the formation of hexagonal Zn NCs[15] nor a crystallization of $MgZn_2O_4$ spinel could be detected in the electron microscopy images. Clearly, a phase separation into ZnO NCs and surrounding MgO host is apparently favored using the coimplantation synthesis method over formation of a solid solution rocksalt $Mg_{1-x}Zn_xO$ phase previously observed in deposited thin films.[2–4]

Finally, Fig. 3 shows the evolution of optical absorption spectra for a representative coimplanted sample as a function of annealing stage. A clear signature of the optical band edge of rocksalt ZnO NCs grows in near ~2.8 eV (estimated from the position of maximum slope of the edge) upon thermal annealing, reaching maximum intensity after annealing at 870–970 K. Previous OAS studies on rocksalt $Mg_{1-x}Zn_xO$ solid solutions and pressure-induced rocksalt ZnO thin films allowed us to extract the position of the optical band gap of ~3.0–3.2 eV (Refs. 2 and 3) and ~2.5 eV (Ref. 5), respectively, which corresponds well with the present observations. The band edge absorption disappears completely after annealing at 1170 K, coinciding with the dissociation of the ZnO NCs which dissolve into the MgO matrix, similar to that observed for Zn NCs by monitoring the Mie resonance for a Zn-implanted sample annealed in the same batch.

This study demonstrates that coimplantation and thermal annealing provide a straightforward synthesis route for ZnO nanocrystals in MgO. The stabilization of the rocksalt phase is governed by the small lattice mismatch with MgO giving rise to correspondingly low interface energies. The observed lattice matching will furthermore provide the benefit of good passivation of surface states. Favorable kinetics is induced by the initially abundant presence of vacancies in the implantation layer. Combined, this results in the nucleation and growth of ZnO NCs in MgO, in contrast to the formation of a solid solution observed for deposited films. Future challenges include the doping of these embedded NCs, which could be incorporated in the synthesis process by using an additional implantation step,[27] and tailoring of monodisperse NC size distributions inducing optical band gap tunability, enabling a wide range of applications in integrated (opto-) electronics, spintronics, and scintillator technology.

This paper is dedicated to the memory of the young Professor K. Saarinen, who passed away December 2005. We thank Dr. F. Tuomisto and Professor K. Saarinen, Helsinki University of Technology, for providing the wurtzite ZnO sample and stimulating discussions.

[1] D. C. Look, Mater. Sci. Eng., B **80**, 383 (2001).
[2] S. Choopun, R. D. Vispute, W. Yang, R. P. Sharma, T. Venkatesan, and H. Shen, Appl. Phys. Lett. **80**, 1529 (2002).
[3] J. Chen, W. Z. Shen, N. B. Chen, D. J. Qui, and H. Z. Wu, J. Phys.: Condens. Matter **15**, L475 (2003).
[4] M. Kunisu, I. Tanaka, T. Yamamoto, T. Suga, and T. Mizoguchi, J. Phys.: Condens. Matter **16**, 3801 (2004).
[5] A. Segura, J. A. Sans, F. J. Manjón, A. Muñoz, and M. J. Herrera-Cabrera, Appl. Phys. Lett. **83**, 278 (2002).
[6] A. Seko, F. Oba, A. Kuwabara, and I. Tanaka, Phys. Rev. B **72**, 024107 (2005).
[7] J. E. Jaffe and A. C. Hess, Phys. Rev. B **48**, 7903 (1993).
[8] A. P. Alivisatos, J. Phys. Chem. **100**, 13226 (1996).
[9] K. Jacobs, J. Wickham, and A. P. Alivisatos, J. Phys. Chem. B **106**, 3759 (2002).
[10] S. W. H. Eijt, A. van Veen, H. Schut, P. E. Mijnarends, A. B. Denison, B. Barbiellini, and A. Bansil, Nat. Mater. **5**, 23 (2006).
[11] M. A. van Huis, A. van Veen, H. Schut, S. W. H. Eijt, B. J. Kooi, and J. Th. M. de Hosson, Acta Mater. **53**, 1301 (2005).
[12] C. V. Falub, P. E. Mijnarends, S. W. H. Eijt, M. A. van Huis, A. van Veen, and H. Schut, Phys. Rev. B **66**, 075426 (2002).
[13] A. L. Roest, J. J. Kelly, D. Vanmaekelbergh, and E. A. Meulenkamp, Phys. Rev. Lett. **89**, 036801 (2003).
[14] P. Huber, H. Karl, and B. Stritzker, Appl. Phys. Lett. **88**, 203123 (2006).
[15] M. A. van Huis, A. van Veen, H. Schut, B. J. Kooi, J. Th. M. de Hosson, X. S. Du, T. Hibma, and R. Fromknecht, Nucl. Instrum. Methods Phys. Res. B **216**, 390 (2004).
[16] J. F. Ziegler, J. P. Biersack, and U. Littmark, *The Stopping and Range of Ions in Solids (TRIM)* (Pergamon, New York, 1985).
[17] A. van Veen, H. Schut, and P. E. Mijnarends, in *Positron Beams and their Applications*, edited by P. G. Coleman (World Scientific, Singapore, 2000), p. 191.
[18] P. J. Schultz, and K. G. Lynn, Rev. Mod. Phys. **60**, 701 (1988).
[19] B. J. Kooi, A. van Veen, J. Th. M. de Hosson, H. Schut, A. V. Fedorov, and F. Labohm, Appl. Phys. Lett. **76**, 1110 (2000).
[20] J. Xu, J. Moxom, S. H. Overbury, C. W. White, A. P. Mills, Jr., and R. Suzuki, Phys. Rev. Lett. **88**, 175502 (2002).
[21] M. J. Puska and R. M. Nieminen, Rev. Mod. Phys. **66**, 841 (1994).
[22] M. A. van Huis, A. van Veen, H. Schut, C. V. Falub, S. W. H. Eijt, P. E. Mijnarends, and J. Kuriplach, Phys. Rev. B **65**, 085416 (2002).
[23] F. Tuomisto, V. Ranki, K. Saarinen, and D. C. Look, Phys. Rev. Lett. **91**, 205502 (2003).
[24] M. A. van Huis, A. van Veen, H. Schut, B. J. Kooi, and J. Th. M. de Hosson, Phys. Rev. B **67**, 235409 (2003).
[25] M. A. van Huis, A. V. Fedorov, A. van Veen, C. V. Falub, S. W. H. Eijt, B. J. Kooi, J. Th. M. de Hosson, T. Hibma, and R. L. Zimmerman, Nucl. Instrum. Methods Phys. Res. B **191**, 442 (2002).
[26] O. Zhakarov, A. Rubio, and M. L. Cohen, Phys. Rev. B **51**, 4926 (1995).
[27] Y. Kanemistu, H. Matsubara, and C. W. White, Appl. Phys. Lett. **81**, 535 (2002).